Long-Term Forecasting of Internet Backbone Traffic

Konstantina Papagiannaki, *Member, IEEE*, Nina Taft, *Member, IEEE*, Zhi-Li Zhang, *Member, IEEE*, and Christophe Diot

***Abstract*—We introduce a methodology to predict *when and where* link additions/upgrades have to take place in an Internet protocol (IP) backbone network. Using simple network management protocol (SNMP) statistics, collected continuously since 1999, we compute aggregate demand between any two adjacent points of presence (PoPs) and look at its evolution at time scales larger than 1 h. We show that IP backbone traffic exhibits visible long term trends, strong periodicities, and variability at multiple time scales. Our methodology relies on the wavelet multiresolution analysis (MRA) and linear time series models. Using wavelet MRA, we smooth the collected measurements until we identify the *overall long-term trend*. The fluctuations around the obtained trend are further analyzed at multiple time scales. We show that the largest amount of variability in the original signal is due to its *fluctuations at the 12-h time scale*. We model inter-PoP aggregate demand as a multiple linear regression model, consisting of the two identified components. We show that this model accounts for 98% of the total energy in the original signal, while explaining 90% of its variance. Weekly approximations of those components can be accurately modeled with low-order autoregressive integrated moving average (ARIMA) models. We show that forecasting the long term trend and the fluctuations of the traffic at the 12-h time scale yields accurate estimates for at least 6 months in the future.**

***Index Terms*—Autoregressive integrated moving average (ARIMA), capacity planning, network provisioning, time series models, traffic forecasting.**

I. Introduction

INTERNET protocol (IP) network capacity planning is a very important task that has received little attention in the research community. The capacity planning theory for traditional telecommunication networks is a well explored area [1], which has limited applicability in a packet-based network such as the Internet. It normally depends on the existence of a traffic matrix, identifying the amount of traffic flowing between any source to any destination of the network under investigation. Moreover, it requires accurate modeling of the incoming traffic, as well as accurate predictions of its future behavior. The previous information is then combined in a network simulation to identify the points where future upgrades will be needed.

This approach cannot be used in the environment of an IP backbone network because 1) direct measurement of an IP traffic matrix is not possible today and statistical inference techniques [2], [3] have not yet reached levels of accuracy that meet a carrier's target error rates, 2) we do not really know how to model the incoming traffic of a backbone network, and 3) simulating such a large scale network is typically not feasible.

The current best practice in the area is based on the experience and the intuition of the network operators. Moreover, it usually relies on marketing information regarding projected number of customers at different locations within the network. Given provider-specific oversubscription ratios, and traffic assumptions, the operators estimate the impact that the additional customers may have on the network-wide load. The points where link upgrades will take place are selected based on experience, and/or current network state. For instance links that currently carry larger volumes of traffic are likely to be upgraded first.

Our goal is to enhance the previous practices using historical network measurements collected with the simple network management protocol (SNMP). The intuition behind our approach is to use mathematical tools to process historical information and extract trends in the traffic evolution at different time scales. This approach requires the collection of network measurements over long periods of time.

In this paper, we analyze three years of SNMP information collected throughout a major tier-1 IP backbone. Correlating those measurements with topological information, we calculate the aggregate traffic between any two adjacent points of presence (PoPs) and track its evolution over time. We explore the properties of these time series, and propose a methodology that can be applied to forecast network traffic volume months in the future.

Our methodology relies on wavelet multiresolution analysis (MRA) and linear time series models. Initial observations on the traffic reveal strong periodicities, evident long term trends, and variability at multiple time scales. We use wavelets to smooth out the original signal until we identify the overall long term trend. The fluctuations of the traffic around the obtained trend are further analyzed at multiple time scales. This analysis reveals that 98% of the energy in the signal is captured by two main components, namely the long term trend, and the fluctuations at the 12-h time scale. Using the analysis of variance (ANOVA) technique, we further show that a multiple linear regression model containing the two identified components can explain 90% of the signal's variance.

We model the weekly approximations of the two components using autoregressive integrated moving average (ARIMA) models, and develop a prediction scheme that is based on their forecasted behavior. We show that forecasting network backbone traffic based on our model can yield accurate estimates for at least 6 months in the future. Moreover, with a minimal

Manuscript received January 19, 2004; revised March 13, 2005. The work of Z.-L. Zhang was supported in part by the National Science Foundation under Grants ANI-0073819, ITR-0085824, and CAREER Award NCR-9734428.

K. Papagiannaki and C. Diot are with Sprint ATL, Intel Research, Cambridge CB3 0FD, U.K. (e-mail: dina.papagiannaki@intel.com; christophe.diot@intel.com).

N. Taft is with Sprint ATL, Intel Research, Berkeley, CA 94704 USA (e-mail: nina.taft@intel.com).

Z.-L. Zhang is with the University of Minnesota, Minneapolis, MN 55455 USA (e-mail: zhzhang@cs.umn.edu).

Digital Object Identifier 10.1109/TNN.2005.853437

computational overhead, and by modeling only the long term trend and the fluctuations of the traffic at the 12-h time scale, we produce estimates which are within 5%–15% of the actual measured behavior.

Our methodology combined with actual backbone traffic measurements leads to different forecasting models for different parts of the network. Our results indicate that different PoP-pairs exhibit different rates of growth and experience different types of fluctuations. This illustrates the importance of defining a methodology for deriving models as opposed to developing a single model for inter-PoP aggregate traffic flows.

Lastly, we show that trends in Internet data may change over time for short or long periods of time. We acknowledge that forecasting a dynamic environment imposes challenges to forecasting techniques that rely on stationarity. Consequently, we complete our work by proposing a scheme for the detection of "extreme" (and perhaps erroneous) forecasts, that are due to short-lived (e.g., on the order of a few months) network changes. We provide the network operator with recommended values in place of these "extreme" forecasts and show that uncertainty in forecasts can be addressed through the analysis of historical trends and impacts both the edge as well as the core of the network.

The remainder of the paper is structured as follows. In Section II, we present previous efforts at forecasting Internet traffic. Our objectives are listed in Section III. In Section IV, we present the data analyzed throughout the paper and make some initial observations. Section V provides an overview of the wavelet MRA, along with results of its application on our measurements. Forecasts are derived using linear time series models, presented in Section VI. We evaluate our approach in Section VII. The trends modeled in the data may in fact change through time. In Section VIII, we acknowledge the fact that the Internet is a dynamic environment and propose a scheme to identify "extreme" forecasts due to changes in the network configuration. We conclude in Section IX.

II. Related Work

An initial attempt toward long-term forecasting of IP network traffic is described in [4]. The authors compute a single value for the aggregate number of bytes flowing over the National Science Foundation Network (NSFNET), and model it using linear time series models. They show that the time series obtained can be accurately modeled with a low-order ARIMA model, offering highly accurate forecasts (within 10% of the actual behavior) for up to two years in the future.

However, predicting a single value for the future network-wide load is insufficient for capacity planning purposes. One needs to pinpoint the areas in the network where overload may occur in order to identify the locations where future provisioning will be required. Thus, per-node or per-link forecasts are required. The authors of [4] briefly address this issue, mentioning that initial attempts toward this direction did not prove fruitful.

Other work in the domain of Internet traffic forecasting typically addresses small time scales, such as seconds or minutes, that are relevant for dynamic resource allocation [5]–[10]. To the best of our knowledge, our work is the first to model the evolution of IP backbone traffic at large time scales, and to develop models for long-term forecasting that can be used for capacity planning purposes.

III. Objectives

The "capacity planning" process consists of many tasks, such as addition or upgrade of specific nodes, addition of PoPs, and expansion of already existing PoPs. For the purposes of this work, we use the term "capacity planning" only to refer to the process of upgrading or adding links between two PoPs in the core of an IP network.

The core of an Internet service provider (ISP) backbone network is usually overprovisioned and consists of very high speed links, i.e., OC-48, OC-192. Those links are a rather large part of a network operator's investment and have a provisioning cycle between 6 and 18 months. Therefore, the capability to forecast *when and where* future link additions or upgrades will have to take place would greatly facilitate network provisioning.

In order to address the issue of *where* upgrades or additions should take place, we measure and forecast aggregate traffic between adjacent PoPs. In that way carriers can determine which pair of PoPs may need additional interconnecting capacity. There are a number of factors that influence *when* an upgrade is needed. These factors include service level agreements with customers, network policies toward robustness to failures, the rate of failures, etc. We assume that carriers have a method for deciding how many links should interconnect a given pair of PoPs and the acceptable levels of utilization on these links. Once carriers articulate a utilization threshold beyond which traffic levels between PoPs are considered prohibitive, one can schedule an upgrade before these levels are actually exceeded. Our task is to predict when in the future the traffic levels will exceed these acceptable thresholds.

In this paper, we use historical information collected continuously since 1999 on the Sprint IP backbone network. There are many factors that contribute to trends and variations in the overall traffic. Our measurements come from a highly dynamic environment reflecting events that may have short or long-lived effects on the observed behavior. Some of the events that may have a long-lived effect include changes in the network topology and in the number of connected customers. These events influence the overall long-term trend, and the bulk of the variability observed. Events that may have a short-lived effect include link failures, breaking news or flash crowd events, as well as denial of service attacks. These events normally have a direct impact on the measured traffic but their effect wears out after some time. As a consequence, they are likely to contribute to the measured time series with values which lie beyond the overall trend. Given that such events are very hard to predict, and are already taken into account in the calculation of the threshold values that will trigger upgrades, as described earlier in this section, we will not attempt to model them in this paper.

IV. Measurements of Inter-PoP Aggregate Demand

We now describe the measurements collected and analyzed throughout the paper. We present some initial observations

about Internet traffic at time scales larger than 1 h. These observations motivate the approach used throughout the rest of the paper.

A. Data Collected and Analysis

We collect values for two particular management information base (MIB) objects, incoming and outgoing link utilization in bps, for all the links of all the routers in the Sprint IP backbone throughout a period that spans from 1999 until the end of 2003. This operation yields traces from more than 2000 links, some of which may not be active anymore. The values collected correspond to an exponentially weighted moving average computed on 10-s link utilization measurements. The exponential weighted average has an average age of 5 min and allows for more recent samples to be weighted more heavily than samples earlier in the measurement interval.[1]

Along with the SNMP data, we collect topological information. This information is collected several times per day by an agent downloading configuration information from every router in the network. It contains the names of the routers in each PoP, along with all their active links, and their destinations. Therefore, it allows us to identify those links in the SNMP data set that interconnect specific PoPs in the network.

We correlate the SNMP data with the topological information, and derive aggregate demand, in bps, between any two adjacent PoPs. In this procedure, we need to address two issues. Firstly, the collection is not synchronized, i.e., not all links are polled at the same time to avoid overload at the collection station. Second, the collection is not reliable [SNMP messages use user datagram protocol (UDP)] as their transport protocol), i.e., we may not have one record for each 5-min interval for every link in the network. As a consequence, the derivation of the aggregate demand is performed as follows.

- For each link in the SNMP data, we identify its source and destination PoP. We use the notation $l_{sd}(k)$ to denote the kth link connecting PoP s to PoP d.
- Time is discretized in 90-min intervals. We denote time intervals with index t. The reasons why we selected intervals of 90-min are provided in Section V-A.
- The aggregate demand for any PoP-pair (s, d) at time interval t is calculated as the sum of all the records obtained at time interval t from all links k in $\{l_{sd}(k)\}$, divided by the number of records. This metric gives the *average aggregate demand of a link* from PoP s to PoP d at time interval t.

This approach allows us to handle the case of missing values for particular links in the aggregate flow. Moreover, it does not suffer from possible inaccuracies in the SNMP measurements, since such events are smoothed out by the averaging operation. With the aforementioned procedure we obtain 169 time series (one for each pair of adjacent PoPs in our network). For the remainder of the paper we focus our discussion on eight of those. These are the longest traces at our disposal which also correspond to highly utilized paths throughout the network. In the following sections, we look into their properties, and devise techniques for forecasting their values in the medium (i.e., months ahead) and long-term future (i.e., 6 months).

[1]Because these objects belong to a proprietary MIB, we have no further information about how this average value is calculated.

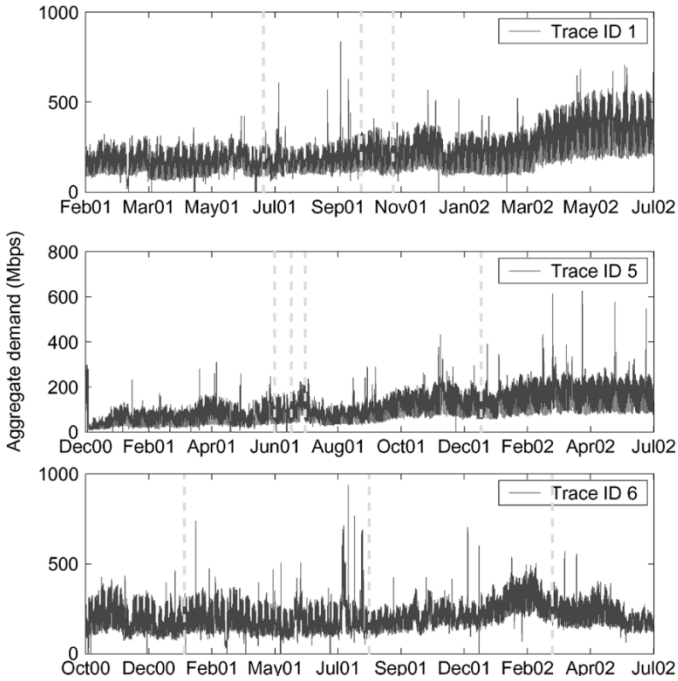

Fig. 1. Aggregate demand between two adjacent PoPs in Mb/s for Traces 1, 5, and 6. The upper two plots demonstrate an increase in the amount of traffic exchanged between the two PoPs. The vertical lines identify the points in time when additional links were provisioned for the interconnection of the two PoPs, and are rarely preceded by evident increase in the carried traffic due to long provisioning cycles.

B. Initial Observations

In Fig. 1, we present the aggregate demand for three PoP pairs in our network. The time series span from the end of 2000 until July 2002 and capture the activity of a multiplicity of links whose number may increase in time. Vertical bars identify the time when additional links became active in the aggregate. As can be seen, link additions are rarely preceded by a visible rise in the carried traffic. This behavior is due to the long provisioning cycles.

From the same figure, we can see that different PoP pairs exhibit different behaviors as far as their aggregate demand is concerned. A *long term trend* is clearly visible in the traces. For Trace 1, and 5, this trend is increasing with time, while for Trace 6 it looks more constant with a sudden shift in January 2002, that lasts for 2 months.

Shorter-term fluctuations around the overall long term trend are also present across all traces, and manifest themselves in different ways. For instance, Trace 1 shows an increasing *deviation* around its long term trend. On the other hand, Trace 6 exhibits smaller fluctuations, that look consistent over time.

Regardless of the differences observed in the three traces, one common property is the presence of large spikes throughout them. Those spikes correspond to average values across 90 minutes, which indicate a surge of traffic in that particular interval that is high or constant enough to have a significant effect on a 90-min average. Such spikes may correspond to link failures, which reroute part of the affected traffic onto this particular path,

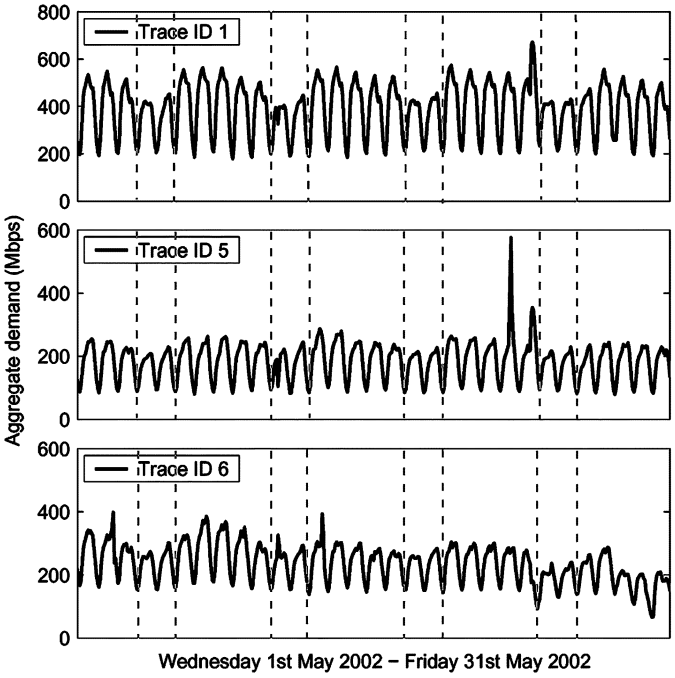

Fig. 2. Aggregate demand between the pairs of PoPs presented in Fig. 1 for the month of May 2002 (Traces 1, 5, and 6). Traffic exhibits strong diurnal patterns. Weekend traffic, for the two days between dashed lines, may differ from weekday traffic but such a phenomenon is not evident across all three traces.

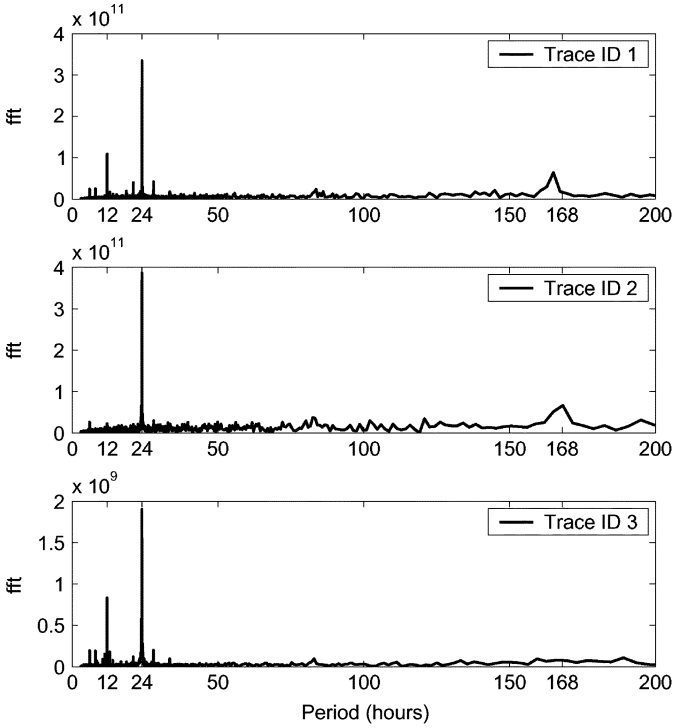

Fig. 3. Fast Fourier transform of aggregate demand for Trace 1–3. The strongest cycle in the data is the one of the day, e.g., 24 h. Certain traces may also exhibit strong periodicities at the weekly or the 12-h cycle.

routing changes, or even denial of service attacks. As mentioned in Section II, we decide to treat those spikes as outliers. This does not mean we ignore the data but simply that we do not attempt to model or predict these spikes.

In Fig. 2, we present a detail of Fig. 1, which corresponds to the month of May 2002. This figure indicates the presence of strong daily and weekly cycles. The drop in traffic during the weekend (denoted by the dashed lines) may be substantial as in Trace 1, smaller as in Trace 5, or even nonexistent as in parts of Trace 6.

From the previous observations it is clear that there are strong periodicities in the data. In order to verify their existence, we calculate the Fourier transform for the eight traces at our disposal. Results indicate that the dominant period across all traces is the 24-h one. Other noticeable periods correspond to 12, and 168 h (i.e., weekly period). Fig. 3 presents the fast Fourier transform for three of the traces, demonstrating that different traces may be characterized by different periodicities.[2]

In summary, initial observations from the collected time series lead to three main findings: 1) there is a multitimescale variability across all traces (traces vary in different ways at different time scales), 2) there are strong periodicities in the data, and 3) the time series exhibit evident long-term trends, i.e., nonstationary behavior. Such findings can be exploited in the forecasting process. For instance, periodicities at the weekly cycle imply that the time series behavior from one week to the next can be predicted. In the next section, we address these three points.

[2]Trace 5, and 6, presented in the previous figures, exhibit similar behavior to Trace 1. However, for Trace 6, the weekly period is stronger than the 12-h one.

V. Multitimescale Analysis

In this section, we analyze the collected measurements at different time scales. We show that using the wavelet MRA we can isolate the underlying overall trend, and those time scales that significantly contribute to its variability.

A. Wavelet MRA Overview

The wavelet MRA describes the process of synthesizing a discrete signal by beginning with a very low resolution signal (at the coarsest time scale) and successively adding on details to create higher resolution versions of the same signal [11]–[13]. Such a process ends with a complete synthesis of the signal at the finest resolution (at the finest time scale). More formally, at each time scale 2^j, the signal is decomposed into an *approximate* signal (or simply, *approximation*) and a *detailed* signal through a series of scaling functions $\phi_{j,k}(t)$ and wavelet functions $\psi_{j,k}(t)$, where $k \in Z$ is a time index at scale j. The scaling and wavelet functions are obtained by dilating and translating the mother scaling function $\phi(t), \phi_{j,k}(t) = 2^{-j/2}\phi(2^{-j}t - k)$, and the mother wavelet function $\psi(t), \psi_{j,k}(t) = 2^{-j/2}\psi(2^{-j}t - k)$. The approximation is represented by a series of (scaling) coefficients $a_{j,k}$, and the detail by a series of (wavelet) coefficients $d_{j,k}$.

Consider a signal (time series) $x(t)$ with N data points at the finest time scale. Using MRA, $x(t)$ can be written as

$$x(t) = \sum_{k \in Z} a_{p,k}\phi_{p,k}(t) + \sum_{0 \le j \le p} \sum_{k \in Z} d_{j,k}\psi_{j,k}(t) \qquad (1)$$

where $p \le \log N$. The sum with coefficients $a_{p,k}$ represents the approximation at the coarsest time scale 2^p, while the sums with

coefficients $d_{j,k}$ represent the details on all the scales between 0 and p.

Using the signal processing parlance, the roles of the mother scaling and wavelet functions $\phi(t)$ and $\psi(t)$ can be described and represented via a low-pass filter h and a high-pass filter g [13]. Consequently, the MRA and synthesis of a signal $x(t)$ can be implemented efficiently as a filter bank. The approximation at scale j, $\{a_{j,k}\}$, is passed through the low-pass filter h and the high-pass filter g to produce the approximation $\{a_{j+1,k}\}$ and the detail $\{d_{j+1,k}\}$ at scale $j+1$. Note that at each stage, the number of coefficients at scale j is decimated into half at scale $j+1$, due to downsampling. This decimation reduces the number of data points to be processed at coarser time scales, but also leaves some "artifacts" in coarser time scale approximations.

More recently, the so-called à-trous wavelet transform has been proposed, which produces "smoother" approximations by filling the "gap" caused by decimation, using redundant information from the original signal [14], [15]. Under the à-trous wavelet transform, we define the approximations of $x(t)$ at different scales as

$$c_0(t) = x(t) \tag{2}$$

$$c_j(t) = \sum_{l=-\infty}^{\infty} h(l) c_{j-1}(t + 2^{j-1} l) \tag{3}$$

where $1 \leq j \leq p$, and h is a low-pass filter with compact support. The detail of $x(t)$ at scale j is given by

$$d_j(t) = c_{j-1}(t) - c_j(t). \tag{4}$$

Let $d_j = \{d_j(t), 1 \leq t < N\}$ denote the wavelet coefficient at scale j, and $c_p = \{c_p(t), 1 \leq t < N\}$ denote the signal at the lowest resolution, often referred to as the residual. Then the set $\{d_1, d_2, \ldots, d_p, c_p\}$ represents the wavelet transform of the signal up to the resolution level p, and the signal $x(t)$ can be expressed as an expansion of its wavelet coefficients

$$x(t) = c_p(t) + \sum_{j=1}^{p} d_j(t). \tag{5}$$

At this point we can justify our decision about averaging our measurements across 90-min intervals. We know that using the wavelet MRA we can look into the properties of the signal at time scales 2^j times coarser than the finest time scale. Furthermore, the collected measurements exhibit strong periodicities at the cycle of 12 and 24 h. Using 1.5 h as the finest time scale allows us to look into the behavior of the time series at the periods of interest by observing its behavior at the third $(2^3 \times 1.5 = 12)$ and fourth $(2^4 \times 1.5 = 24)$ time scale.

B. MRA Application on Inter-PoP Aggregate Demands

For the smoothing of our data we chose as the low-pass filter h in (3) the B_3 spline filter, defined by $(1/16, 1/4, 3/8, 1/4, 1/16)$. This is of compact support (necessary for a wavelet transform), and is point-symmetric. Symmetric wavelets have the advantage of avoiding any phase shifts; the wavelet coefficients do not "drift" relative to the original signal. The B_3 spline filter gives at each resolution level a signal which is much smoother than the one at the previous level without distorting possible periodicities in the data, and preserving the original structure. The B_3 spline filter has been previously used in time series smoothing in [16]–[18].

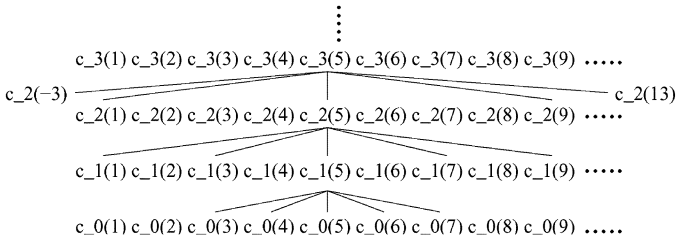

Fig. 4. Illustration of the à-trous wavelet transform. Each level corresponds to a particular time scale; the first level corresponds to the time scale of the original signal and the approximation becomes coarser as we move upward in the figure. The coefficients of a particular level are computed based on the elements of the previous level. As the time scale becomes coarser the elements used from the previous level are farther apart from each other.

In order to understand how $c_j(t)$ is computed at each time scale j, we schematically present in Fig. 4 how $c_1(5), c_2(5)$, and $c_3(5)$ are calculated according to (3), and the B_3 spline filter. Element $c_1(5)$ is computed based on the values $c_0(t) = x(t)$ at times $(5-2), (5-1), 5, (5+1)$, and $(5+2)$. Then, we can calculate $c_2(5)$, based on $c_1(1), c_1(3), c_1(5), c_1(7)$, and $c_1(9)$. Notice that moving toward coarser levels of resolution we need values from the previous resolution level which are farther apart from each other. For this reason, this wavelet transform is called the à-trous wavelet transform, which means "with holes." One important point we should make is that $c_p(t)$ is defined for each $t = 1, 2, \ldots, n$, where n corresponds to 1.5-h intervals and is limited by the size N of the original signal. According to (3), computing $c_p(n)$ requires values of c_{p-1} until time $n + 2^p$, which iteratively requires values of c_{p-2} until time $n+2^{p-1}$, etc. As a consequence, the calculation of $c_p(n)$ requires the original time series $x(t)$ to have $n + \sum_{j=1}^{j=p} 2^j$ values. Given that our original signal contains N values, our wavelet coefficients up to the sixth resolution level will contain n values, where $n + \sum_{j=1}^{j=6} 2^j = N$, or $n = N - 126$.

In Figs. 5 and 6, we present the approximation and detail signals for Trace 5 at each time scale, when it is analyzed up to resolution level $2^6 = 96$ h. We chose to use the sixth time scale as our coarsest time scale because it provides a sufficiently smooth approximation signal. In addition, given that it is the greatest power of 2 that leads to a number of hours smaller than the number of hours in a week (i.e., 168 h), it captures the evolution of the time series from one week to the next without the effect of the fluctuations at the 12 and 24 h time scale. Fig. 5 clearly shows how the wavelet MRA smooths out the original signal. Visual inspection of the derived detail signals in Fig. 6 further suggests a difference in the amount of variability that each one contributes.

Given the derived decomposition, we calculate the energy apportioned to the overall trend (c_6) and each one of the detail signals. The energy of a signal $y(t), 1 \leq t \leq N$, is defined as $E = \sum_{t=1}^{N} y^2(t)$. Table I shows that the overall trend c_6 accounts for 95% to 97% of the total energy. We then subtract the overall trend c_6 from the data, and study the amount of energy distributed among the detail signals. Fig. 7 shows that across all eight traces in our study, there is a substantial difference in the

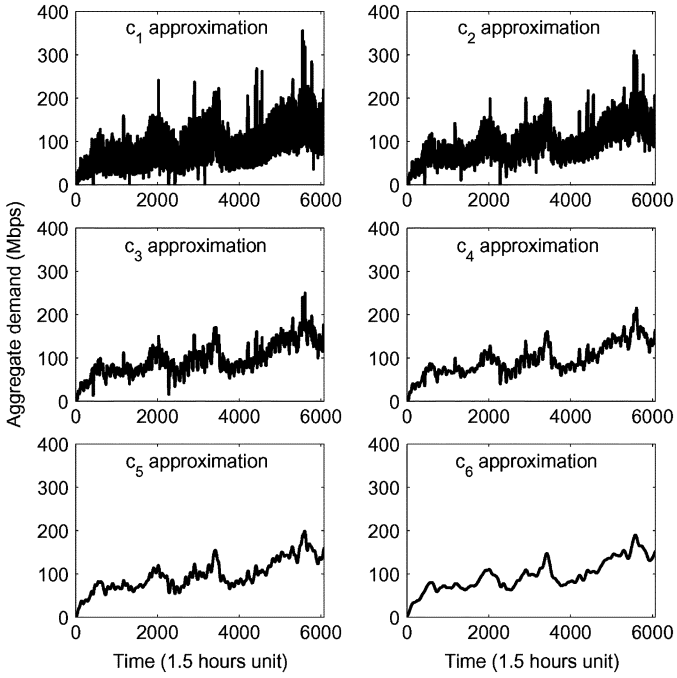

Fig. 5. Six approximation signals for the inter-PoP aggregate demand of Trace 5. The signals have been obtained through wavelet MRA based on the à-trous wavelet transform. The sixth time scale corresponds to 96 h.

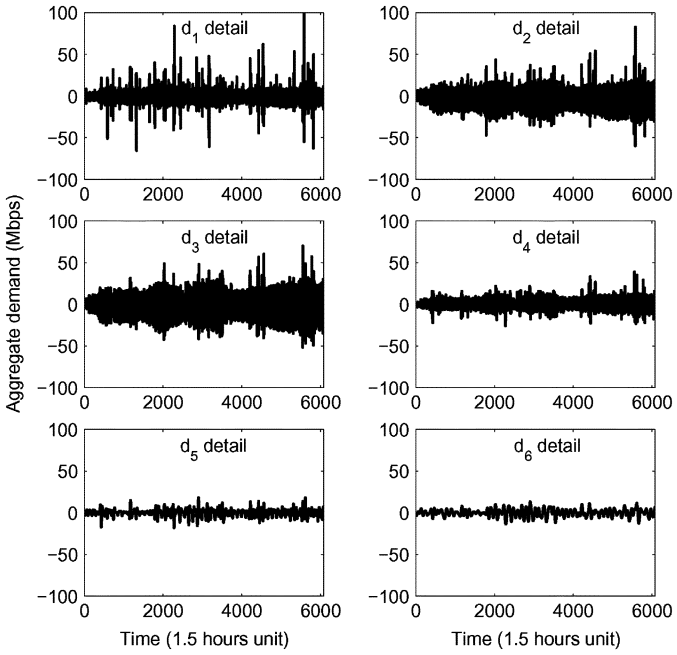

Fig. 6. Six detail signals for the inter-PoP aggregate demand of Trace 5. The signals have been obtained through wavelet MRA based on the à-trous wavelet transform. The sixth time scale corresponds to 96 h.

amount of energy in the detail signals. Moreover, the maximum amount of energy in the details is always located at the third time scale, which corresponds to the fluctuations across 12 h. Approximating the original signal as the long term trend, c_6, and the fluctuations at the 12-h time scale, d_3, is further capable of accounting for 97% to 99% of the total energy (Table I).

TABLE I
PERCENTAGE OF TOTAL ENERGY IN c_6, AND $c_6 + d_3$

Trace ID	1	2	3	4
c_6	96.07%	97.20%	95.57%	96.56%
$c_6 + d_3$	98.10%	98.76%	97.93%	97.91%
Trace ID	5	6	7	8
c_6	95.12%	95.99%	95.84%	97.30%
$c_6 + d_3$	97.54%	97.60%	97.68%	98.45%

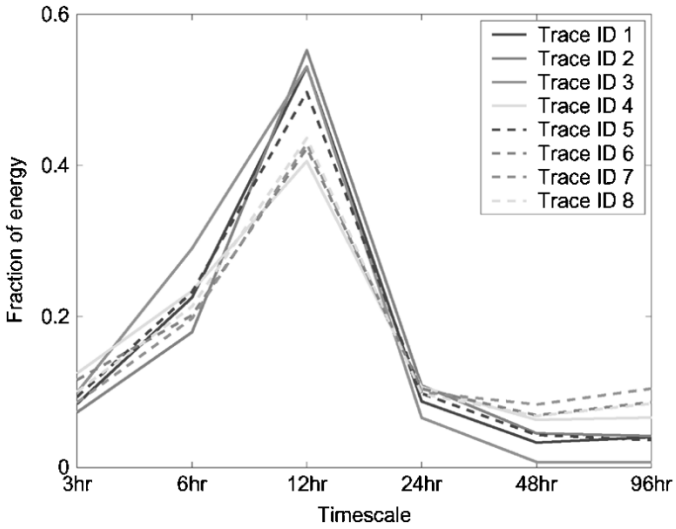

Fig. 7. Energy distribution for the detail signals. The majority of the energy accumulated in the detail signals is concentrated in the detail signal at the 12-h time scale.

In the next section, we look into the properties of the signals derived from the wavelet MRA with respect to the variance they account for in the overall signal.

C. Analysis of Variance (ANOVA)

As explained in Section V-A, the original signal can be completely reconstructed using the approximation signal at the sixth time scale, and the six detail signals at lower time scales. The model defined in (5) can also be conceived as a multiple linear regression model, where the original signal $x(t)$ is expressed in terms of its coefficients.

The ANOVA technique is a statistical method used to quantify the amount of variability accounted for by each term in a multiple linear regression model [19]. Moreover, it can be used in the reduction process of a multiple linear regression model, identifying those terms in the original model that explain the most significant amount of variance.

Using the ANOVA methodology we calculate the amount of variance in the original signal explained by the sixth approximation signal and each one of the detail signals. The results indicate that the detail signals d_1, d_2, d_5, and d_6 contribute less than 5% each in the variance of the original signal.

Ideally, we would like to reduce the model of (5), to a simple model of two parameters, one corresponding to the overall long term trend, and a second one accounting for the bulk of the variability. Possible candidates for inclusion in the model, except from the overall trend c_6, are the signals d_3 and d_4. We know that the detail signal d_3 carries the majority of the energy among

TABLE II
ANOVA RESULTS FOR ALL EIGHT TRACES

Trace ID	1	2	3	4
β	2.09	2.06	2.11	2.23
R^2	0.87	0.94	0.89	0.87
Trace ID	5	6	7	8
β	2.12	2.18	2.13	2.16
R^2	0.92	0.80	0.86	0.91

all the detail signals. Thus, one possible reduced model is the following:

$$x(t) = c_6(t) + \beta d_3(t) + e(t). \tag{6}$$

Using least squares, we calculate the value of β for each one of the traces at our disposal. All traces led to a β estimate between 2.1 and 2.3 (Table II). Using ANOVA, we test how representative the model of (6) is with respect to the proportion of variance it explains [19].

If $x(t)$ is the observed response, and $e(t)$ is the error incurred in (6), we define SSE $= \sum_{t=1}^{n} e(t)^2$ (sum of squares error). The total sum of squares (SST) is defined as the uncertainty that would be present if one had to predict individual responses without any other information. The best one could do is predict each observation to be equal to the sample mean. Thus, we set SST $= \sum_{t=1}^{n}(x(t)-\bar{x})^2$. The ANOVA methodology partitions this uncertainty into two parts. One portion is accounted for by the model. It corresponds to the reduction in uncertainty that occurs when the regression model is used to predict the response. The remaining portion is the uncertainty that remains even after the model is used. We define SSR as the difference between SST and SSE. This difference represents the sum of the squares explained by the regression. The fraction of the variance that is explained by the regression, SSR/SST, determines the goodness of the regression and is called the "coefficient of determination," R^2. The model is considered to be statistically significant if it can account for a large fraction of the variability in the response, i.e., yields large values for R^2. In Table II, we present the results obtained for the value of β, and R^2 for all eight traces.

The reduced model is capable of explaining 80% to 94% of the variance in the signal. Moreover, if we decide to include the term d_4 in the model of (6), the results on R^2, presented in Table II, are only marginally improved, and increased by 0.01 to 0.04.

D. Summary of Findings From MRA and ANOVA

From the wavelet MRA, we draw three main conclusions:

- there is a clear overall long-term trend present in all traces;
- the fluctuations around this long term trend are mostly due to the significant changes in the traffic bandwidth at the time scale of 12 h;
- the long term trend and the detail signal at the third time scale account for approximately 98% of the total energy in the original signal.

From the ANOVA, we further conclude that:

- the largest amount of variance in the original signal can be explained by its long term trend c_6 and the detail signals d_3, and d_4 at the time scales of 12 and 24 h, respectively;
- the original signal can be sufficiently approximated by the long term trend and its third detail signal. This model explains approximately 90% of the variance in the original signal.

Based on those findings, we derive a generic model for our time series, presented in (7). This model is based on (6), where we set $\beta = 3$, for a model valid across the entire backbone. We use a value for β that is slightly greater than the values listed in Table II since slight overestimation of the aggregate traffic may be beneficial in a capacity planning setting

$$x'(t) = c_6(t) + 3d_3(t). \tag{7}$$

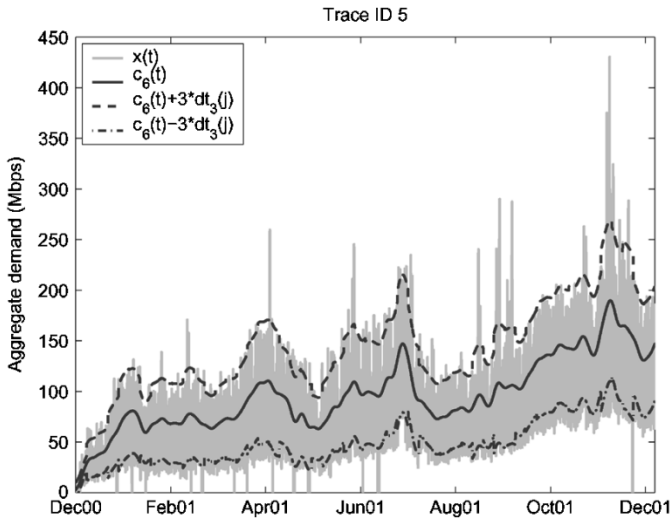

Fig. 8. Approximation of the original signal x(t) using $c_6(t)$ that captures the long term trend and $dt_3(j)$ that captures the average daily standard deviation within a week. Signal $c_6(t) \pm 3 * dt_3(t)$ exposes the weekly variation in traffic without including outliers that mainly correspond to unpredictable events. The time series is defined for each 90-min interval.

E. Implications for Modeling

For forecasting purposes at the time scale of weeks and months, one may not need to accurately model all the short term fluctuations in the traffic. More specifically, for capacity planning purposes, one only needs to know the traffic baseline in the future along with possible fluctuations of the traffic around this particular baseline.

Component $d_3(t)$ in the model of (7) is defined for every 90-min interval in the measurements capturing in time the short-term fluctuations at the time scale of 12 h. Given that the specific behavior within a day may not be that important for capacity planning purposes, we calculate the standard deviation of d_3 within each day. Furthermore, since our goal is not to forecast the exact amount of traffic on a particular day months in the future, we calculate the weekly standard deviation $dt_3(j)$ as the average of the seven values computed within each week. Such a metric represents the fluctuations of the traffic around the long term trend from day to day within each particular week.

In Fig. 8, we show the aggregate demand for Trace 5, as calculated from the SNMP data. In the same figure, we plot the long term trend in the data, along with two curves showing the approximation of the signal as the sum of the long term trend

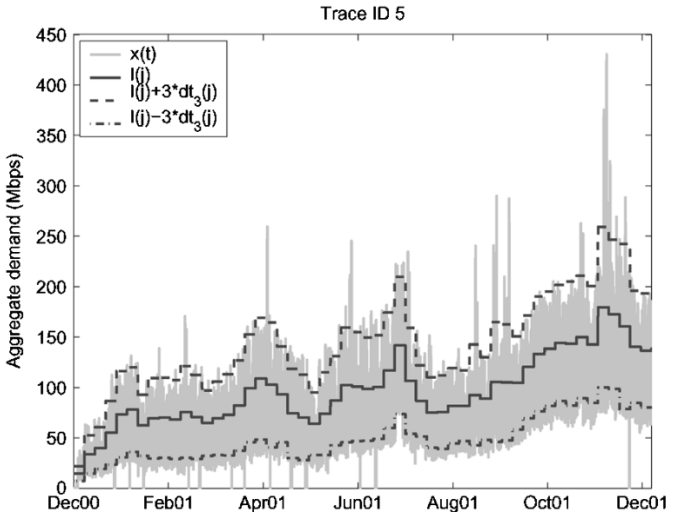

Fig. 9. Approximation of the signal using the average weekly long term trend $l(j)$ and the average daily standard deviation within a week $dt_3(j)$. Signal $l(j) \pm 3 * dt_3(j)$ tracks the changes in the original signal $x(t)$ while operating at the time scale of 1 week. Compact representation of the collected time series allows for efficient processing.

plus and minus three times the average daily standard deviation within a week. We see that approximating the original signal in such a way exposes the fluctuations of the time series around its baseline with very good accuracy.

Notice that the new signal dt_3 features one value every week, exposing the average daily standard deviation within the week. Similarly, we can approximate the long term trend with a more compact time series featuring one value for every week. Given that the sixth approximation signal is a very smooth approximation of the original signal, we calculate its average across each week, and create a new time series $l(j)$ capturing the long term trend from one week to the next. The forecasting process will have to predict the behavior of

$$\hat{x}(j) = l(j) + 3dt_3(j) \tag{8}$$

where j denotes the index of each week in our trace.

The resulting signal is presented in Fig. 9. We confirm that approximating the original signal using weekly average values for the overall long term trend, and the daily standard deviation results in a model which accurately captures the desired behavior.

In the next section, we introduce the linear time series models, and show how they can help derive forecasts for the two identified components. Once we have those forecasts, we compute the forecast for the original time series and compare it with collected measurements.

VI. Time Series Analysis Using the ARIMA Model

A. Overview of Linear Time Series Models

Constructing a time series model implies expressing X_t in terms of previous observations X_{t-j}, and noise terms Z_t which typically correspond to external events. The noise processes Z_t are assumed to be uncorrelated with a zero mean and finite variance. Such processes are the simplest processes, and are said to have "no memory," since their value at time t is uncorrelated with all the past values up to time $t-1$.

Most forecasting models described in the literature are linear models. From those models, the most well-known are the autoregressive (AR), moving average (MA), and autoregressive moving average (ARMA) models.

A time series X_t is an ARMA(p,q) process if X_t is stationary and if for every t

$$X_t - \phi_1 X_{t-1} - \cdots - \phi_p X_{t-p} = Z_t + \theta_1 Z_{t-1} + \cdots + \theta_q Z_{t-q}$$

where $Z_t \sim WN(0,\sigma^2)$ and the polynomials $(1-\phi_1 z - \cdots - \phi_p z^p)$ and $(1+\theta_1 z + \cdots + \theta_q z^q)$ have no common factors [20]. If $p=0$, then the model reduces to a pure MA process, while if $q=0$, the process reduces to a pure AR process.

This equation can also be written in a more concise form as

$$\phi(B)X_t = \theta(B)Z_t \tag{9}$$

where $\phi(\cdot)$, and $\theta(\cdot)$ are the pth and qth degree polynomials, and B is the backward shift operator $(B^j X_t = X_{t-j}, B^j Z_t = Z_{t-j}, j = 0, \pm 1, \ldots)$.

The ARMA model fitting procedure assumes *the data to be stationary*. If the time series exhibits variations that violate the stationary assumption, then there are specific approaches that could be used to render the time series stationary. The most common one is what is often called the "differencing operation." We define the lag-1 difference operator ∇ by

$$\nabla X_t = X_t - X_{t-1} = (1-B)X_t \tag{10}$$

where B is the backward shift operator as already introduced. If the non stationary part of a time series is a polynomial function of time, then differencing finitely many times can reduce the time series to an ARMA process.

An ARIMA$(\mathrm{p},\mathrm{d},\mathrm{q})$ model is an ARMA(p,q) model that has been differenced d times. Thus, it has the form

$$\phi(B)(1-B)^d X_t = \theta(B)Z_t, \quad Z_t \sim WN(0,\sigma^2) \tag{11}$$

If the time series has a nonzero average value through time, then the previous equation also features a constant term μ on its right-hand side.

B. Time Series Analysis of the Long-Term Trend and Deviation

In order to model the obtained components $l(j)$ and $dt_3(j)$ using linear time series models, we have to separate the collected measurements into two parts: 1) one part used for the estimation of the model parameters, and 2) a second part used for the evaluation of the performance of the selected model. Since our intended application is capacity planning, where traffic demand has to be predicted several months ahead in the future, we select the estimation and evaluation periods such that the latter contains 6 months of data.

For each one of the analyzed traces, we use the measurements collected up to January 15, 2002 for the modeling phase, and the measurements from January 16, 2002 until July 1, 2002 for the evaluation phase. Given that not all time series are of the same duration, the isolation of the last 6 months for evaluation purposes may lead to specific traces featuring a small number of measurements for the estimation phase. Indeed, after posing this

TABLE III
ARIMA MODELS FOR THE LONG TERM TREND

ID	Order	Model	μ	σ^2
T1	(0,1,2)	$X(t) = X(t-1) + Z(t) - 0.1626Z(t-1) - 0.4737Z(t-2)$	0.5633E+06	0.2794E+15
T4	(0,1,1)	$X(t) = X(t-1) + Z(t) + 0.4792Z(t-1)$	0.4155E+06	0.1339E+15
T5	(0,1,1)	$X(t) = X(t-1) + Z(t) + 0.1776Z(t-1)$	0.2301E+07	0.1516E+15
T6	(0,1,2)	$X(t) = X(t-1) + Z(t) - 0.3459Z(t-1) - 0.4578Z(t-2)$	0.7680E+06	0.6098E+15
T8	(0,1,1)	$X(t) = X(t-1) + Z(t) + 0.2834Z(t-1)$	0.2021E+07	0.1404E+16

TABLE IV
ARIMA MODELS FOR THE WEEKLY DEVIATION

ID	Order	Model	μ	σ^2
T1	(0,1,1)	$X(t) = X(t-1) + Z(t) - 0.6535Z(t-1)$	0.3782E+05	0.2024E+14
T4	(2,0,0)	$X(t) = 0.8041X(t-1) - 0.3055X(t-2) + Z(t)$	0.1287E+08	0.7295E+13
T5	(0,1,1)	$X(t) = X(t-1) + Z(t) - 0.1493Z(t-1)$	0.3094E+06	0.8919E+13
T6	(3,0,0)	$X(t) = 0.3765X(t-1) - 0.1964X(t-2) - 0.2953X(t-3) + Z(t)$	0.2575E+08	0.3057E+14
T8	(0,1,1)	$X(t) = X(t-1) + Z(t) - 0.5565Z(t-1)$	0.3924E+05	0.4423E+14

requirement three out of the eight traces in our analysis (Trace 2, 3, and 7) consist of less than 6 months of information. Such limited amount of information in the estimation period does not allow for model convergence. As a consequence, we continue our analysis on the five traces remaining.

We use the Box-Jenkins methodology to fit linear time series models [20]. Such a procedure involves the following steps: i) determine the number of differencing operations needed to render the time series stationary, ii) determine the values of p, and q in (9), iii) estimate the polynomials ϕ, and θ, and iv) evaluate how well the derived model fits the data. For the model fitting we used both Splus [21] and ITSM [20], and obtained similar results. The estimation of the model parameters is done using Maximum Likelihood Estimation. The best model is chosen as the one that provides the smallest Akaike information criterion corrected (AICC), Bayesian information criterion (BIC), and forward protection error (FPE) measures [20], while offering the smallest mean square prediction error 6 months ahead. Due to space constraints, we will not go into details about the metrics used in the quality evaluation of the derived model, and refer the reader to [20]. One point we should emphasize is that metrics like AICC, and BIC not only evaluate the fit between the values predicted by the model and actual measurements, but also penalize models with large number of parameters. Therefore, the comparison of the derived models against such metrics leads to the most parsimonious models fitting the data.

C. Models for $l(j)$, and $dt_3(j)$

The computed models for the long term trend $l(j)$ indicate that the first difference of those time series (i.e., the time series of their changes) is consistent with a simple MA model with one or two terms (i.e., $d = 1, q = 1$ or $d = 1, q = 2$), plus a constant value μ (Table III). The need for one differencing operation at lag 1, and the existence of term μ across all the models indicate that the long-term trend across all the traces is a simple exponential smoothing process with growth. The trajectory for the long-term forecasts will typically be a line, whose slope is equal to μ. For instance, for Trace 1 the long-term forecast will correspond to a weekly increase of 0.5633 Mb/s. This forecast corresponds to the average aggregate demand of a link in the aggregate. The weekly increase in the total demand between two adjacent PoPs can, thus, be estimated through the multiplication of this value with the total number of active links in the aggregate. Given the estimates of μ across all models in Table III we conclude that all traces exhibit upward trends, but grow at different rates.

Applying the Box-Jenkins methodology on the deviation measurements, we see that for some traces the deviation $dt_3(j)$ can be expressed with simple AR models (Trace 4, and 6), while the remaining can be accurately modeled as MA processes after one differencing operation (Table IV). Therefore, the deviation for Traces 1, 5, and 8 increases with time (at rates one order of magnitude smaller than the increase in their long term trends), while the deviation for Traces 4 and 6 can be approximated with a weighted moving average, which indicates slower evolution. These results confirm earlier observations on Fig. 1 in Section IV-B.

From the previous tables we see that one cannot come up with a single network-wide forecasting model for the inter-PoP aggregate demand. Different parts of the network grow at different rates (long-term trend), and experience different types of variation (deviation from the long-term trend). Our methodology extracts those trends from historical measurements and can identify these PoP pairs in the network that exhibit higher growth rates and, thus, may require additional capacity in the future.

At this point we should note that the Box-Jenkins methodology could also have been applied on the original time series $x(t)$. However, given the existence of three strong periods in the data (which would require a seasonal ARIMA model with three seasons [20]), the variability of the time series at multiple time scales, the existence of outliers, and the size of the original time series, such an approach leads to highly inaccurate forecasts, while being extremely computationally intensive. Our technique is capable of isolating the overall long term trend and identifying those components that significantly contribute to its variability. Predictions based on weekly approximations of those components provide accurate estimates with a minimal computational overhead. All forecasts were obtained in seconds.

In the next section, we use the derived models for the weekly prediction of the aggregate traffic demands. Then forecasts are compared against actual measurements.

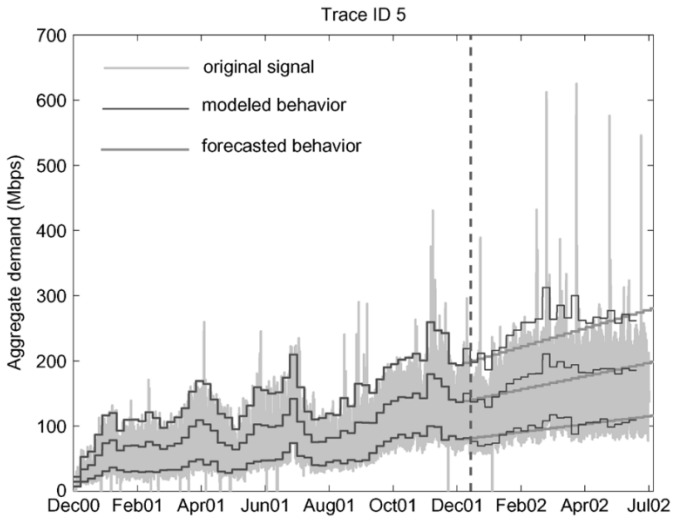

Fig. 10. 6-months forecast for Trace 5 as computed on January 15, 2002. Forecasts are provided for 1) the long term trend and 2) the modeled signal that also takes into account 95% of the variability in the original signal. The time series model is trained on data from Dec. 2000 until Dec. 2001, capturing the behavior of the signal without the effect of outliers.

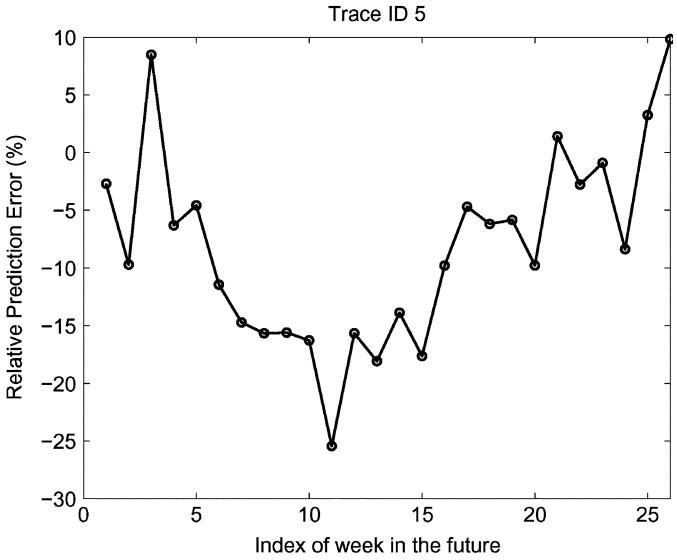

Fig. 11. Weekly relative prediction error for Trace 5 when forecasts are generated for 6 months in the future. The prediction error fluctuates around zero indicating that there is no consistent under- or over-estimation effect. The average absolute error is approximately 10%.

VII. Evaluation of Forecasts

Using our models we predict a baseline aggregate demand for a particular week in the future, along with possible deviations around it. The overall forecast for the inter-PoP aggregate demand is then calculated based on (8). For the remainder of this section we focus on the upper limit of the obtained forecasts, since this is the value that would be used for capacity planning purposes.

In Fig. 10, we present the time series collected until July 1, 2002. On the same figure we present the modeled behavior in the estimation period, and the forecasts in the evaluation period.[3] From visual inspection of the presented plot, one can see that the proposed methodology behaves very well for this particular trace.

In order to be able to quantify the quality of the predictions we have to compare the forecasts against the behavior we model in the measured signal. We, thus, proceed as follows:

- we apply the MRA on the measurements in the evaluation period;
- we calculate the long term trend $l(j)$ and weekly deviation $dt_3(j)$ for each week in the same period;
- we compute $\hat{x}(j)$ based on (8);
- lastly, we calculate the error in the derived forecast as the forecasted value minus $\hat{x}(j)$, divided by $\hat{x}(j)$.

In Fig. 11, we present the relative error between the derived forecast and $\hat{x}(j)$ for each week in the evaluation period. Negative error implies that the actual demand was higher than the one forecasted. As can be seen from the figure, the forecasting error fluctuates with time, but is centered around zero. This means that on average we neither underestimate nor overestimate the aggregate demand. The average prediction error across weeks is -3.6%. Lastly, across all five traces, the average absolute relative prediction error is lower than 15%.

[3]In Fig. 10, the vertical dashed line indicates the beginning of the forecasting period. The three lines in the evaluation period correspond to the forecast of the long-term $l(j)$, and the forecasts for $l(j) + 3dt_3(j), l(j) - 3dt_3(j)$.

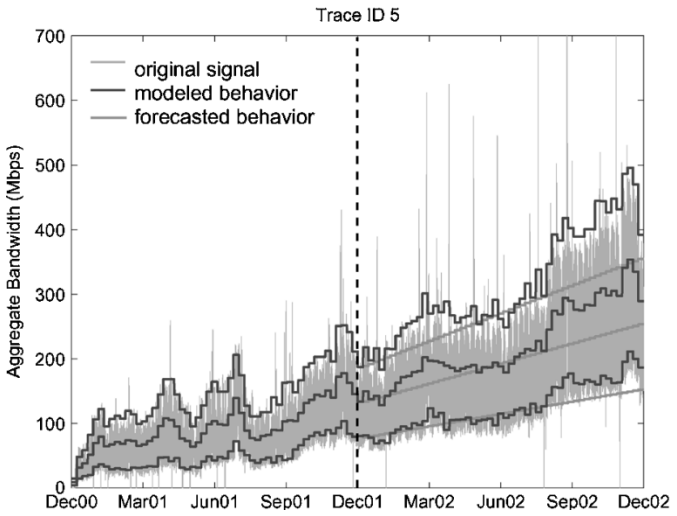

Fig. 12. Yearly forecast for Trace 5 as computed on January 15th, 2002. Forecasts are provided for 1) the long term trend and 2) the modeled signal that also takes into account 95% of the variability in the original signal. The time series model is trained on data from Dec. 2000 until Dec. 2001, capturing the behavior of the signal without the effect of outliers.

Our forecasting models can be used to predict demand for more than 6 months in the future, and identify when the forecasted demand will exceed the operational thresholds that will trigger link upgrades (as explained in Section III). In that case, though forecasts should be used with caution. As is the case with any forecasting methodology, the farther ahead in the future one attempts to predict, the larger the error margin that should be allowed.

In Fig. 12, we present the yearly forecast for Trace 5 along with the measured aggregate traffic flowing between this particular pair of adjacent PoPs. Forecasts, as computed on January 15, 2001, are highly accurate until September 2002 and divert

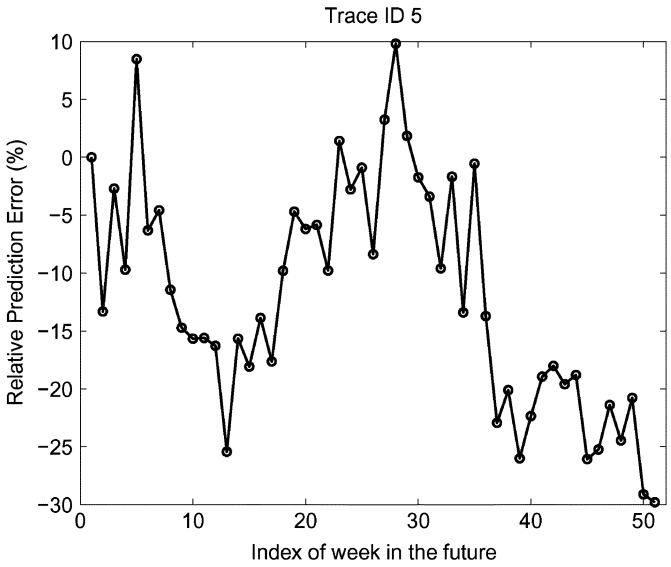

Fig. 13. Weekly relative prediction error for Trace 5 when forecasts are generated for 12 month in the future. The prediction error fluctuates around zero but appears to significantly deviate toward the end of the year.

for the remainder of the year. The reason behind this behavior is that traffic flowing between the analyzed adjacent PoPs experiences significant growth after September 2002.

In terms of relative prediction errors, as shown in Fig. 13, our forecasts are highly accurate for 36 weeks into the future. The average relative prediction error made during this period is approximately -5%. However, our methodology underestimates the amount of aggregate traffic between the two PoPs for the last 10 weeks in the year by approximately 20%, due to the significant increase in traffic. Performing this same type of analysis on all five traces resulted in an average absolute relative prediction error of 17% for the yearly forecasts. Thus, our yearly forecasts are slightly worse than the 6-month forecasts. The reason for that is that the stationarity assumption is more likely to be invalidated across longer periods of time, e.g., it is more likely to observe a change in the network environment in the long-term future.

VIII. Forecasting a Dynamic Environment

The accuracy of the computed traffic forecasts depends upon several factors. First, if the input itself is very noisy, then the long-term and deviation signals will be hard to model, i.e., the trends in this signal will be rather hard to capture in a consistent fashion. Second, sources of error can come from new behaviors, or changes, in the underlying traffic itself. Recall that any forecast is based on models developed from the already seen data. If new behaviors were to emerge, then these might not be captured by the model and could lead to errors in the forecast. There are typically two types of changes that can surface, those that are short-lived (also called *transient* changes), and those that are long-lived (considered more *permanent* changes). In this context, short-lived changes would be those that are on the order of a few weeks while long-lived changes refer to those that are on the order of several months or longer. An Internet backbone is a highly dynamic environment because the customer base is continuously changing and because any ISP's network is under continuous expansion, either via upgrades or the addition of new equipment. If some of these factors occur with some regularity, then they will be reflected in our forecasting model and should not generate prediction errors. However, many of these factors would not necessarily be captured by the model and could generate errors. Hence, the accuracy of our forecasts very much depends on whether the captured trends can still be observed in the future.

Before assessing the impact of such changes on our predictions, we give some examples of these sources of change in dynamic IP backbones. Short-lived changes could be due to changes in routing whereas long-lived changes would be generated from topological changes inside the network. When failures such as fiber cuts happen in the Internet, a common reaction among operators is to shift around the assigned link weights that are used by the IGP protocol for shortest-path routing. Such moves offload traffic from some links, shift it elsewhere thereby increasing the load on other links. Such a routing change can last for a few hours or even a few days, depending upon how long the fiber cut takes to fix. Large amounts of traffic can get shifted around when carriers implement changes to their load balancing policies. Shifting traffic around means that the composition of flows contributing to the aggregate traffic is altered and so the aggregate behavior could change as well. Finally BGP announcements from the edge of the network, could cause new internal routes to be selected when a BGP next hop is altered. Such a change could easily last a few weeks. More permanent changes come from topological changes that usually reflect network expansion plans. For example, the addition of new links, new nodes, or even new customers may lead to changes that may ultimately affect the traffic load and growth on inter-PoP links. Similarly, the removal of links or nodes that are decommissioned may impact the model and the forecast.

To ensure that operators can use our model as a tool, we need to be able to help them identify, when possible, those predictions whose errors might be large. In this section, we define bounds on our predictions and consider predictions outside these bound to be "extreme" forecasts. By identifying extreme forecasts, carriers can choose to ignore them, or not, using their own understanding of what is currently happening in the network. We also explore the issue of whether some links are more error-prone than others.

A. Identification of "Extreme" Forecasts

We now define a simple method that is to be coupled with the main forecasting method to identify those extreme forecasts that should be treated with skepticism. We have a large dataset at our disposal because our forecasting method has been running continuously since September 2002, as part of a capacity planning tool on the Sprint IP backbone network; it computes forecasts for all pairs of adjacent PoPs once a week. Recall that different parts of the network are modeled using different ARIMA models; and in addition, the particular ARIMA model that best fits the collected measurements for a specific pair of adjacent PoPs, can also change over time. As already illustrated, our models do capture a large amount of the regular fluctuations and variability. What we want to identify here are those predictions that may result in errors, not because of traffic variability,

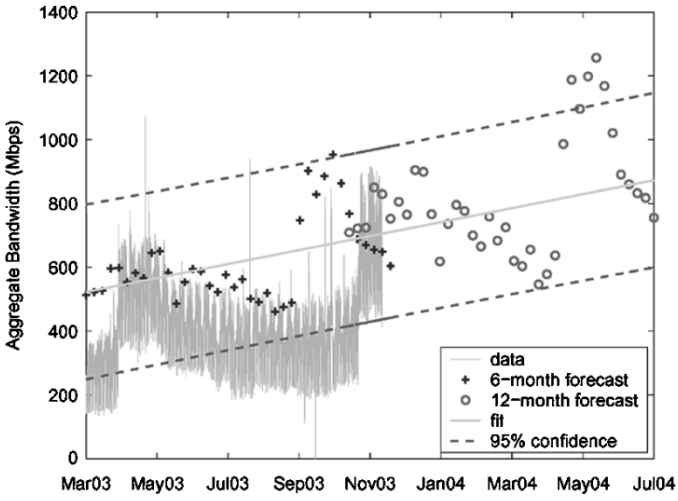

Fig. 14. Visualization of the algorithm used for the detection of "extreme" forecasts. The measured traffic is presented with a solid line. Between March and November 2003 we generate two forecasts, one for the next six and one for the next 12 month. The linear trend in the forecasts along with its 95% confidence interval are able to pinpoint that the forecasts generated for the month of June in 2004 may significantly deviate from "typically observed behavior."

but because of underlying network changes (e.g., routing and/or topological changes).

Each week our tool generates a forecast for the next 6 and 12 months, thus, defining the forecasted growth trend. With over one year's worth of data, we can see how similar an ensemble of predictions are. If the forecasted trend aligns itself (i.e., is within reasonable bounds) with previously forecasted trends, then our confidence on the new forecasts is higher. Otherwise, the new forecasts may be an artifact of short- or long-lived changes.

To devise a scheme for the identification of "extreme" forecasts we proceed as follows. Although we have almost two years worth of data, we only use the weeks between September 2002 and July 2003 to generate forecasts - so that we can compare one year forecasts with actual data. For this period, we compute the predicted aggregate demand for each pair of adjacent PoPs inside the network for the next 6 and 12 months. More specifically, for each week i since November 2002 we compute a forecast l_{i+26} and l_{i+52}, defining the line of forecasted "growth."

In Fig. 14, we present the 6- and 12-month forecasts for Trace 5 that were generated with our methodology for the period of March 2003 and July 2004. Notice that in Fig. 14 we simply denote each forecast with a single point instead of a trend line as in previous figures. In essence, we have abstracted the forecasted trend with 2 points alone, one corresponding to the forecast after 6 months and one to the forecast after 12 months.[4] In the same figure, we also present the actual measurements collected through SNMP with a continuous line. Fig. 14 shows that forecasts until September 2003 agree perfectly with the collected measurements. We notice that forecasts generated through time may diverge from each other depending on the point in time when they were computed. For instance, the 6-month forecasts obtained for October 2003 (based on the data until April 2003) significantly divert from the forecasts obtained for the end of August 2003 (based on data until March 2003). The forecasts generated for the month of October are the result of the spike in traffic observed 6 months earlier, in April 2003, which lasted for 2 months.

"Extreme" forecasts are identified via divergence from typically observed behavior. To quantify what constitutes "typically observed behavior," we use weighted least squares estimation to fit a polynomial through the historical forecasts. We have shown that our ARIMA models typically extract linear trends in the traffic exchanged between PoPs. Therefore, we set the degree of the polynomial function equal to one, and compute the line $y = ax + b$ that best captures the trend among historical forecasts, along with its corresponding 95th confidence interval. We identify extreme forecasts as those that are outside the bounds defined by the 95th confidence interval. As can be seen in Fig. 14, forecasts generated for this particular pair of adjacent PoPs typically follow an increasing trend. The 95th confidence bounds are wide around the fitted line indicating that typical historical forecasts do fluctuate a good deal over time. After having identified an extreme forecast, a network operator can replace this estimate with a slightly more conservative one, that is, the upper bound for the 95th confidence interval. In the example in Fig. 14, the forecasts for the month of July 2004 are considered "extreme" and could be replaced with the upper 95th confidence bound of 1.1 Gbps.

Note that our model adapts itself as it observes more data and, thus, can accommodate (over time) either short-lived or long-lived changes. If an underlying change persists, this will be reflected in the data and ultimately in the model. Thus, forecasts which are considered "extreme" at one moment in time, may in fact start aligning with later forecasts. With persistent change, the slope of the line fitted through the data will adjust its slope and so will the 95th confidence interval bounds. It can happen that forecasts considered "extreme" at some previous point in time become "typical" at some later point in time. This is an advantage of adaptive models.

B. Uncertainty in Forecasts as a Network Artifact

It is now natural to ask whether there is some intrinsic property of a backbone network that makes specific areas harder to forecast. Alternatively, we would like to examine whether specific links inside the network are more error-prone than others, exhibiting trends that are harder to capture consistently over time.

To address these questions, we first explain why one might intuitively think that some links are more susceptible than others. Consider the examples we mentioned previously regarding changes in traffic load induced by either routing or topological changes. In an IP network, traffic flowing between two adjacent PoPs is the result of the multiplexing of different origin-destination (OD) PoP-to-PoP flows, as dictated through routing. An OD PoP-to-PoP flow captures the total amount of traffic that originates at one particular PoP and departs the network at another specific PoP. Each such flow uses at least one path through the network for its traffic. These paths are determined using the intradomain routing protocol in effect (in our case IS-IS). Consequently, the traffic we forecast in this work is the result of the superposition of multiple individual

[4]Note that the cyclic behavior observed in the figure is due to the fact that for each point in time we generate two forecasts corresponding to the next 6 and 12 months, thus, obtaining a measure for the forecasted growth.

OD flows. At each point in time, and depending on the state of the routing regime, the aggregate demand between adjacent PoPs consists of different OD flows whose routes traverse those two particular adjacent PoPs. Therefore, transient changes can occur on an inter-PoP link if its traffic has changed in terms of its constituent OD flows. Routing changes propagated through BGP or changes in the customer population in specific network locations can actually lead to significant changes in the amount of traffic a particular PoP sources or sinks.

If a link is located at the edge of the network, then routing or topological changes across the network will only impact it if they are specific to its edge PoP. On the other hand, if a link is located in the core of the IP network then its load can be affected by routing changes both inside and at the edge of the network. One might, thus, postulate that internal links are more error-prone, or that their forecasts are more uncertain. However, one might also conjecture that internal links have a greater amount of statistical multiplexing going on and that this smooths out uncertainty. To examine whether any of these effects impact one type of link more than another, we define loose metrics to describe the position of a link and its forecasting uncertainty, and examine these two metrics in Sprint's IP backbone.

1) Position of a Link in the Network: For the PoP topology of the entire Sprint IP network we compute all routable paths across the network, i.e., for each PoP we compute all paths to every other PoP. Then, for each link inside the network we compute the position of this link inside every path. If the position of a link is consistently at the beginning or the end of a routable path, we call the link an "edge link", otherwise, we call it an "internal link." In essence, an "internal link" is any link that is used to transit traffic between any two PoPs that are not its endpoints.

2) Uncertainty in Forecasts: To assess whether one can generalize if one of the two broad classes of links is inherently more difficult to forecast, we assemble the 6- and 12-month forecasts for *all* 169 pairs of adjacent PoPs in our study. Note that in our dataset (containing just a little less than two years worth of data), numerous routing and topological changes did occur at various places. Thus, by studying *all* inter-PoP links, these changes should be perceptible somewhere. Using the same approach as shown previously, we again fit a line through the forecasts and compute the "growth slope" (i.e., the value of a). If the forecasts exhibit significant variations, the "growth slope" a will be accompanied by a large confidence interval. If the forecasts show good alignment, then the confidence interval for the "growth" is going to be more contained. If we denote the confidence interval of a as $[a - da, a + da]$, we define "uncertainty in forecast" to be the fraction $(2da/a)$. Notice that this metric is less sensitive to the actual size of the forecast, in contrast to other possible uncertainty indices, such as the width of the 95th confidence interval band shown in Fig. 14.

We first examine our "uncertainty" metric for two particular links inside the network, in Figs. 15 and 16. The first link is an "internal" link and the second is an "edge" link. The forecasts obtained for the "internal" link appear to be less volatile than the forecasts obtained for the approximately equal-activity "edge" link. In this particular case, the uncertainty metric does differentiate the uncertainty of the two different links and indicates that the edge link (with an uncertainty of 0.89) is more volatile in terms of its forecasts than the internal link (with an uncertainty of 0.32).

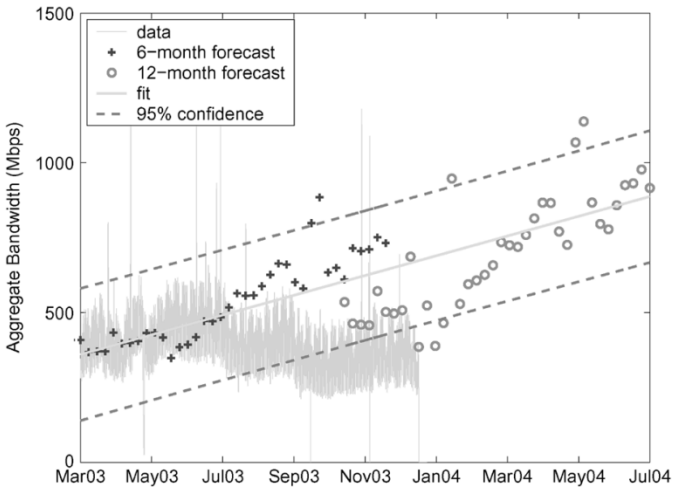

Fig. 15. Uncertainty in forecast generated for an internal link (uncertainty = 0.32). The 95% confidence inteval around the trends in the forecasts is tight.

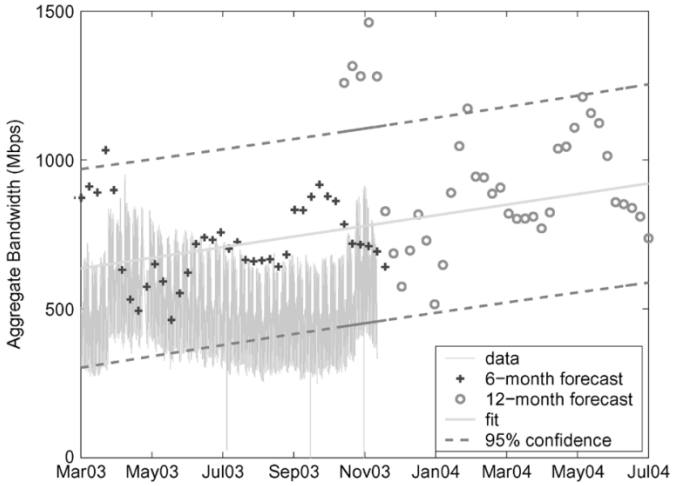

Fig. 16. Uncertainty in forecast generated for an edge link (uncertainty = 0.89). Forecasts fluctuate with time and significantly exceed the 95% confidence interval in the forecasted trend in November 2003. The confidence interval is wide around the fitted trend in the forecasts.

Although our metric does differentiate these two particular links in terms of their uncertainty, we now show that one should be careful not to generalize too quickly, as this observation does not hold when examining *all* links. In Fig. 17, we show two sets of results, one curve for the cumulative density function of the uncertainty of all "internal" inter-PoP links, and a second curve for the "edge" links. We notice that in general there are no significant differences in the forecasting uncertainty of edge and internal links. Hence, the composite effect of the factors inducing change (change in routing, topology and customer base) and factors such as statistical multiplexing do not seem to make

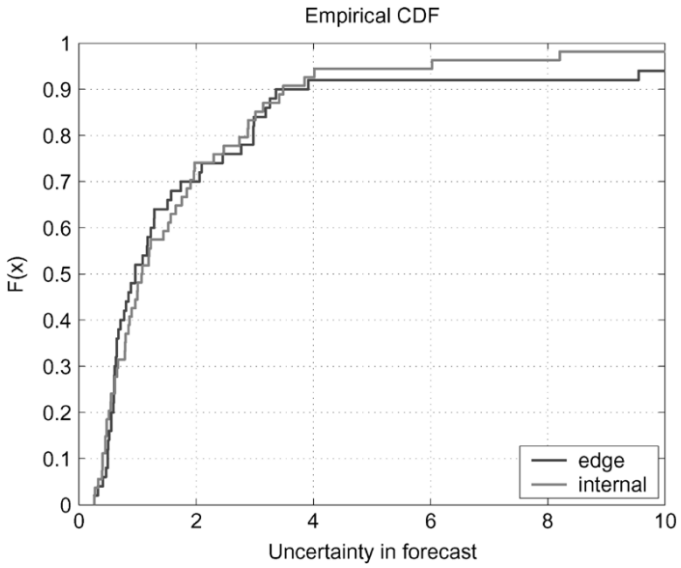

Fig. 17. Empirical cumulative density function for the forecasting uncertainty for "edge" and "internal" links. There appears to be no significant difference between the behavior of the two types of links.

one type of link more error-prone than another.[5] This also illustrates a strength of our method because it shows that our approach is not biased toward one type of link or another. The accuracy of our forecasts does not depend upon the position of the link inside the network.

IX. Conclusion

We presented a methodology for predicting *when and where* link upgrades/additions have to take place in the core of an IP network. We measured aggregate demand between any two neighboring PoPs in the core of a major tier-1 IP network, and analyzed its evolution at time scales larger than 1 h.

We showed that the derived time series exhibit strong periodicities at the cycle of 12, and 24 h, as well as one week. Moreover, they experience variability at multiple time scales, and feature distinct overall long-term trends.

Using wavelet MRA, we isolated the *overall long term trend*, and analyzed variability at multiple time scales. We showed that the largest amount of variability in the signal comes from its *fluctuations at the 12-h time scale*. Our analysis indicates that a parsimonious model consisting of those two identified components is capable of capturing 98% of the total energy in the original signal, while explaining 90% of its variance. The resulting model is capable of revealing the behavior of the network traffic through time, filtering short-lived events that may cause traffic perturbations beyond the overall trend.

We showed that the weekly approximations of the two components in our model can be accurately modeled with low-order ARIMA processes. Our results indicate that different parts in the network grow at different rates, and may also experience increasing deviations from their overall trend, as time progresses. We further showed that calculating future demand based on the forecasted values for the two components in our traffic model yields highly accurate estimates. Our average absolute relative forecasting error is less than 15% for at least 6 month in the future, and 17% across a year.

Acknowledging the fact that the Internet is a dynamic environment, we then addressed the sensitivity of our forecasting scheme to changes in the network environment. We showed that the forecasting models obtained in an operational Tier-1 network may in fact vary in time. In addition, they may capture trends that may not persist. To address this issue, we proposed a scheme for the identification of "extreme" and possibly erroneous forecasts and recommended alternative forecasts in their place. Forecasting a dynamic environment, like the one of an IP backbone network, imposes challenges which are mainly due to topological and routing changes. We showed that such changes appear to impact forecasting of backbone traffic both at the edge as well as the core of the network.

As a concluding remark we emphasize that due to the properties of the collected time series direct application of traditional time series analysis techniques proves cumbersome, computationally intensive and prone to error. Our methodology is simple to implement, and can be fully automated. Moreover, it provides accurate forecasts for at least 6 months in the future with a minimal computational overhead. In this paper, we demonstrated its performance within the context of capacity planning. However, MRA of the original signal and modeling of selected approximation and detail signals using ARIMA models could possibly provide accurate forecasts for the behavior of the traffic at other time scales, such as from one day to the next or at a particular hour on a given day in the future. These forecasts could be useful for other network engineering tasks, like scheduling of maintenance windows or large database network backups.

[5]We acknowledge that one could do a much more detailed study of the impact of such changes, and, thus, our exploration of this issue is preliminary in that we only examined one metric. However our exploration of this metric is comprehensive since we examined *all* inter-PoP links in a large backbone.

Acknowledgment

The authors would like to thank R. Cruz, J.-C. Bolot, P. Thiran, and J.-Y. Le Boudec for their valuable feedback. They would also like to thank A. Goldberg for providing us with the MATLAB code for the wavelet MRA.

References

[1] H. Leijon, "Basic forecasting theories: A brief introduction," ITU, Tech. Rep., Nov. 1998.

[2] A. Medina, N. Taft, K. Salamatian, S. Bhattacharyya, and C. Diot, "Traffic matrix estimation: Existing techniques and new directions," in *Proc. ACM SIGCOMM*, Pittsburgh, PA, Aug. 2002, pp. 161–174.

[3] Y. Zhang, M. Roughan, C. Lund, and D. Donoho, "An information-theoretic approach to traffic matrix estimation," in *Proc. ACM SIGCOMM*, Karlsruhe, Germany, Aug. 2003, pp. 301–312.

[4] N. K. Groschwitz and G. C. Polyzos, "A time series model of long-term NSFNET backbone traffic," in *Proc. IEEE ICC'94*, 1994, pp. 1400–1404.

[5] S. Basu and A. Mukherjee, "Time series models for internet traffic," in *Proc. 24th Conf. Local Computer Networks*, Oct. 1999, pp. 164–171.

[6] J. Bolot and P. Hoschka, "Performance engineering of the world wide web: Application to dimensioning and cache design," in *Proc. 5th Int. World Wide Web Conf.*, May 1996, pp. 185–195.

[7] K. Chandra, C. You, G. Olowoyeye, and C. Thompson, "Non-linear time-series models of ethernet traffic,", CACT, Tech. Rep., Jun. 1998.

[8] R. A. Golding. (1992, Jun.) End-to-end performance prediction for the Internet. CISB, Univ. California, Santa Cruz, CA. [Online]. Available: ftp://ftp.cse.ucsc.edu/pub/tr/ucsccrl-92-26.ps.Z

[9] A. Sang and S. Li, "A predictability analysis of network traffic," in *Proc. INFOCOM*, Tel Aviv, Israel, Mar. 2000, pp. 342–351.

[10] R. Wolski, "Dynamically forecasting network performance using the network weather service," *J. Cluster Comput.*, pp. 119–132, 1999.
[11] I. Daubechies, "Ten lectures on wavelets," in *Proc. Cbms-Nsf Regional Conf. Ser. Applied Mathematics*, vol. 61, 1992.
[12] S. Mallat, "A theory for multiresolution signal decomposition: The wavelet representation," *IEEE Trans. Pattern Anal. Mach. Intell.*, vol. 11, no. 7, pp. 674–693, Jul. 1989.
[13] J. Walker, *A Primer on Wavelets and Their Scientific Applications*. London, U.K.: Chapman & Hall, 1999.
[14] G. Nason and B. Silverman, "The stationary wavelet transform and some statistical applications," in *Lecture Notes in Statistics: Wavelets and Statistics*: citeseer.nj.nec.com/nason95stationary.html, 1995, pp. 281–300.
[15] M. Shensa, "The discrete wavelet transform: Wedding the A Trous and Mallat algorithms," *IEEE Trans. Signal Process.*, vol. 40, no. 10, pp. 2464–2482, Oct. 1992.
[16] J.-L. Starck and F. Murtagh, "Image restoration with noise suppression using the wavelet transform," *Astronomy and Astrophys.*, vol. 288, pp. 342–348, 1994.
[17] A. Aussem and F. Murtagh, "Web traffic demand forecasting using wavelet-based multiscale decomposition," *Int. J. Intell. Syst.*, vol. 16, pp. 215–236, 2001.
[18] P. Yu, A. Goldberg, and Z. Bi, "Time series forecasting using wavelets with predictor-corrector boundary treatment," in *Proc. 7th ACM SIGKDD Int. Conf. Knowledge Discovery and Data Mining*, San Francisco, CA, 2001.
[19] R. Jain, *The Art of Computer Systems Performance Analysis: Techniques for Experimental Design, Measurement, Simulation, and Modeling*. New York: Wiley, 1991.
[20] P. Brockwell and R. Davis, *Introduction to Time Series and Forecasting*: Springer, 1996.
[21] W. N. Venables and B. D. Ripley, *Modern Applied Statistics with SPLUS*. New York: Springer-Verlag, 1999.

Konstantina Papagiannaki (M'02) received the degree in electrical and computer engineering from the National Technical University of Athens, Greece, in 1998 and the Ph.D. degree from the University College London, U.K., in 2003.

From 2000 to 2004, she was a Member of the IP Research Group at the Sprint Advanced Technology Laboratories. She is currently with Intel Research, Cambridge, U.K. Her research interests are in Internet measurements, modeling of Internet traffic, and backbone network traffic engineering.

Nina Taft (M'87) received the B.S degree in computer science from the University of Pennsylvania, Philadelphia, in 1985 and the M.S. and Ph.D. degrees from the University of California at Berkeley in 1990 and 1994, respectively.

From 1995 to 1999, she was a Researcher at SRI International, Menlo Park, CA, working on congestion control and routing in ATM networks. From 1999 to 2003, she was a Senior Researcher at Sprint's Advanced Technology Laboratories, working on Internet measurement, modeling and performance evaluation. In 2003, she joined Intel Research, Berkeley, CA. Her research interests are in traffic and performance measurement, modeling and traffic engineering.

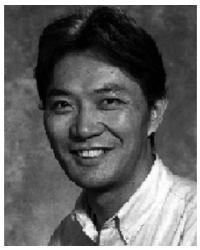

Zhi-Li Zhang (M'97) received the B.S. degree in computer science from Nanjing University, China, in 1986 and the M.S. and Ph.D. degrees in computer science from the University of Massachusetts, Amherst, in 1992 and 1997, respectively. In 1997, he joined the Computer Science and Engineering Faculty at the University of Minnesota, where he is currently an Associate Professor. From 1987 to 1990, he conducted research in the Computer Science Department, Århus University, Denmark, under a fellowship from the Chinese National Committee for Education. He has held visiting positions at Sprint Advanced Technology Labs.; IBM T. J. Watson Research Center; Fujitsu Labs. of America, Microsoft Research China, and INRIA, Sophia-Antipolis, France. His research interests include computer communication and networks, especially the QoS guarantee issues in high-speed networks, multimedia and real-time systems, and modeling and performance evaluation of computer and communication systems.

Christophe Diot received the Ph.D. degree in computer science from INP Grenoble, France, in 1991.

From 1993 to 1998, he was a Research Scientist at INRIA Sophia Antipolis, working on new Internet architecture and protocols. From 1998 to 2003, he was in charge of the IP research at Sprint Advanced Technology Labs. He is currently with Intel Research, Cambridge, U.K. His current interest is measurement techniques and large networks architecture.